Molecular and Cellular Pathobiology

Cancer Research

p53 Is a Direct Transcriptional Target of MYCN in Neuroblastoma

Lindi Chen[1], Nunzio Iraci[3], Samuele Gherardi[3], Laura D. Gamble[1], Katrina M. Wood[2], Giovanni Perini[3], John Lunec[1], and Deborah A. Tweddle[1]

Abstract

MYCN amplification occurs in ~25% of neuroblastomas, where it is associated with rapid tumor progression and poor prognosis. MYCN plays a paradoxical role in driving cellular proliferation and inducing apoptosis. Based on observations of nuclear p53 accumulation in neuroblastoma, we hypothesized that MYCN may regulate p53 in this setting. Immunohistochemical analysis of 82 neuroblastoma tumors showed an association of high p53 expression with MYCN expression and amplification. In a panel of 5 *MYCN*-amplified and 5 nonamplified neuroblastoma cell lines, and also in the Tet21N-regulatable MYCN expression system, we further documented a correlation between the expression of MYCN and p53. In MYCN-amplified neuroblastoma cell lines, MYCN knockdown decreased p53 expression. In Tet21N MYCN+ cells, higher levels of p53 transcription, mRNA, and protein were observed relative to Tet21N MYCN- cells. In chromatin immunoprecipitation and reporter gene assays, MYCN bound directly to a Myc E-Box DNA binding motif located close to the transcriptional start site within the p53 promoter, where it could initiate transcription. E-Box mutation decreased MYCN-driven transcriptional activation. Microarray analysis of Tet21N MYCN+/– cells identified several p53-regulated genes that were upregulated in the presence of MYCN, including *MDM2* and *PUMA*, the levels of which were reduced by MYCN knockdown. We concluded that MYCN transcriptionally upregulates p53 in neuroblastoma and uses p53 to mediate a key mechanism of apoptosis. *Cancer Res; 70(4); 1377–88. ©2010 AACR.*

Introduction

Neuroblastoma is an embryonal malignancy derived from precursor cells of the sympathetic nervous system. Despite significant advances in understanding the biology of this tumor, it currently still remains one of the most difficult childhood cancers to cure, with <40% of patients with high risk disease (stage 4 disease over 18 months of age or *MYCN*-amplified disease) being long-term survivors (1, 2).

Amplification of *MYCN* occurs in ~25% of neuroblastomas, and is associated with rapid tumor progression and poor prognosis (reviewed in ref. 3). MYCN belongs to the *Myc* family of basic-helix-loop-helix-leucine zipper transcription factors that have a critical role in cellular proliferation, differentiation, apoptosis, and oncogenesis. Members of this family function as heterodimers with Max, and exert transcriptional activity by specifically binding to consensus E-Box motifs (CA(C/T)GTG) located within the promoter regions of a diverse set of target genes (reviewed in ref. 4). In contrast to c-MYC, which is expressed in a wide variety of embryonic and adult tissues, MYCN expression is limited to the developing nervous system and selected other sites.

Several genes have been identified as c-MYC transcriptional targets (5),[4] however, less is known about target genes of MYCN. Early studies found that several c-MYC target genes were expressed in some neuroblastoma cell lines with *MYCN* amplification, but not all, suggesting that other cell-specific factors may be important (6). Recent studies have reported significant overlap between c-MYC and MYCN-regulated gene sets (7, 8). Enhanced ectopic expression of MYCN leads to both accelerated cell cycle progression and sensitization to apoptosis, therefore, mechanisms which minimize or evade MYCN-driven apoptosis are essential for tumor progression in neuroblastomas with *MYCN* amplification (reviewed in ref. 9).

p53, often referred to as the "guardian of the genome", is mutated in up to 60% of many human malignancies. In neuroblastoma, p53 is rarely mutated, however, protein accumulation is frequently observed in both neuroblastoma tumors

Authors' Affiliations: [1]Northern Institute for Cancer Research, Newcastle University, [2]Department of Cellular Pathology, Royal Victoria Infirmary, Newcastle upon Tyne, United Kingdom; and [3]Department of Biology, University of Bologna, Bologna, Italy

Note: Supplementary data for this article are available at Cancer Research Online (http://cancerres.aacrjournals.org/).

Corresponding Author: Deborah A. Tweddle, Newcastle University, Northern Institute for Cancer Research, Paul O'Gorman Building, The Medical School, Newcastle University, Framlington Place, Newcastle upon Tyne, NE2 4HH, United Kingdom. Phone: 44-191-246-4421; Fax: 44-191-246-4301; E-mail: D.A.Tweddle@newcastle.ac.uk.

doi: 10.1158/0008-5472.CAN-09-2598

[4] http://www.myc-cancer-gene.org/site/mycTargetDB.asp

and cell lines (reviewed in ref. 10). The presence of accumulated p53 in neuroblastoma has been suggested to be due to the embryonic nature of these tumors, reflecting a failure of the precursor cells to mature (11). We and others have shown that the accumulated p53 is both predominantly nuclear and functional in neuroblastoma tumors and cell lines (reviewed in ref. 12).

Early studies using reporter gene assays and electrophoretic gel mobility analysis reported that p53 was a direct target gene of c-MYC (13, 14). Furthermore, it was shown using

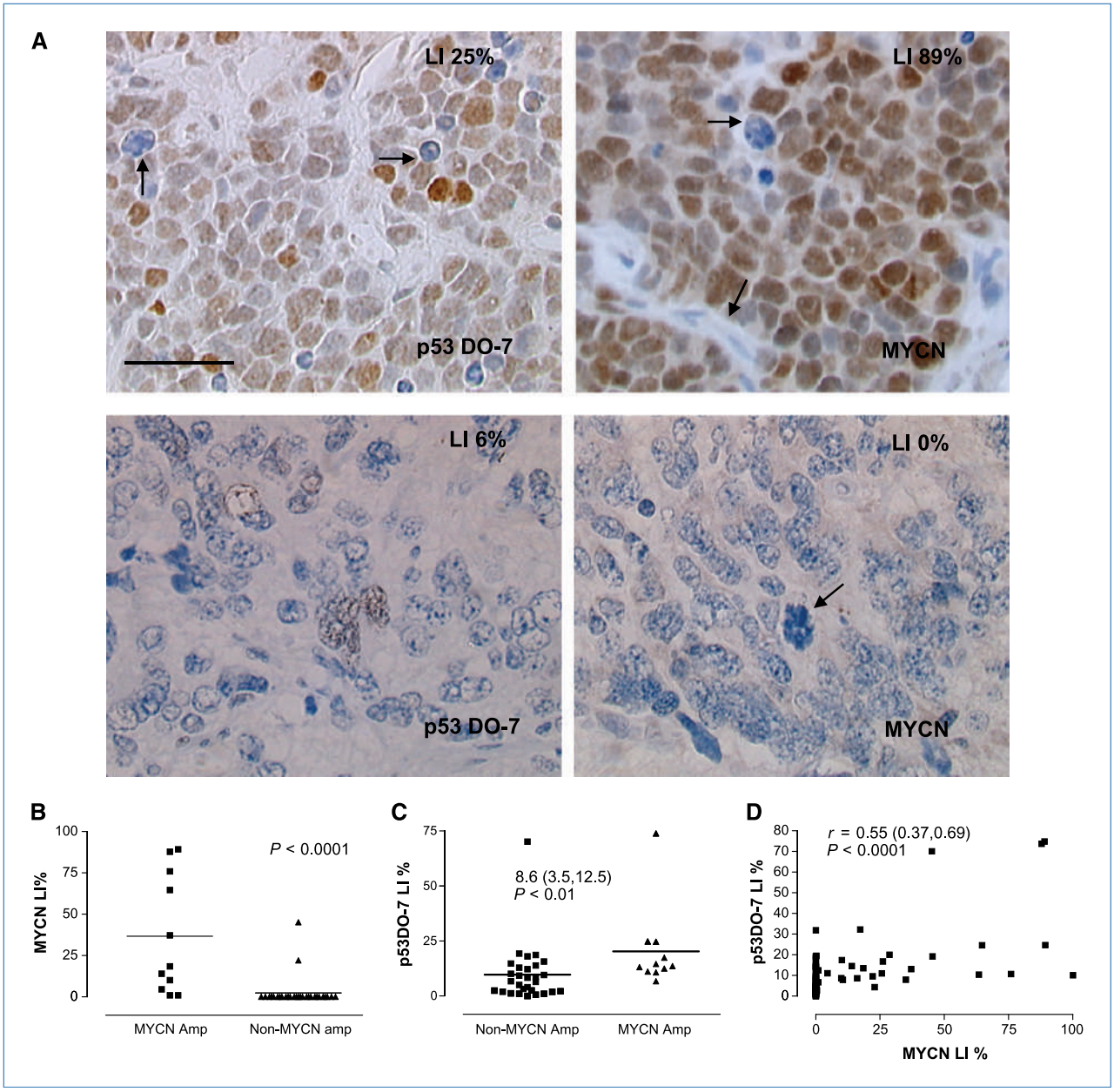

Figure 1. p53 expression is associated with *MYCN* amplification and MYCN protein expression in untreated neuroblastoma tumors. A, top, immunohistochemistry of a stroma-poor, undifferentiated, *MYCN*-amplified, stage 4 primary neuroblastoma, using p53DO-7 antibody (left) showing heterogeneous nuclear immunostaining, absent in apoptotic cells (arrow) and MYCN antibody (right) showing heterogeneous nuclear immunostaining with negative stroma and negative mitotic and apoptotic cells (arrows). Bottom, immunohistochemistry of a stroma-poor nodule of a non–*MYCN*-amplified, stage 4 primary nodular ganglioneuroblastoma, using p53DO-7 antibody (left) showing low-level nuclear immunostaining and MYCN antibody (right) showing absent immunostaining and a mitotic cell (arrow). Top right, labeling indices (LI) for antibodies. Scale bar, 50 μm. B and C, scatter plots of labeling indices showing median expression (two-tailed Mann-Whitney tests used) *MYCN* amplification versus MYCN (B) labeling index, and *MYCN* amplification versus p53DO-7 (C) labeling index (median difference shown and 95% confidence interval). D, correlation between p53DO-7 labeling index and MYCN labeling index (Spearman correlation and 95% confidence interval).

Table 1. *MYCN* amplification and expression is associated with p53 protein expression in 82 neuroblastomas

	Median LI, % (range)	MYCN (*n* = 82)		*P*	*MNA** (*n* = 40)		*P*
		–	+		+	–	
MYCN	>0 (0–100)	–			0	26	**<0.001**
		+			11	3	
p53 DO-7	8 (0–75)	–35	6	**<0.001**	1	14	**<0.05**
		+17	24		10	15	
p53 DO-1	7 (0–89)	–34	5	**<0.001**	1	15	**<0.05**
		+17	25		10	13	
p53 1801	2 (0–20)	–38	10	**<0.001**	2	14	0.2
		+14	20		9	15	

*Fisher's exact, two-sided test. All other parameters χ^2 used. *MNA* = *MYCN* amplification. The median labeling index (LI) for all 82 tumors was used as a cutoff for positive and negative expression (range).

quiescent fibroblasts that p53 directly mediates c-MYC–induced apoptosis, and suggests that c-MYC–driven p53-mediated apoptosis acts as a safeguard mechanism against aberrant oncogenic activation (15). The p53 promoter contains a noncanonical E-Box (CATGTG) located upstream of the transcription initiation site (13, 14) and is recognized by MYC-MAX heterodimers (16), which can bind and initiate transcription (14). Several studies have reported a positive correlation between c-MYC expression and p53 expression in both cell lines and tumors, and that inhibition of c-MYC expression using either antisense RNA or inhibitory peptides led to a decrease in p53 expression (reviewed in ref. 17).

This study set out to test the hypothesis that p53 accumulation in neuroblastoma correlates with *MYCN* amplification status and MYCN expression, and that p53 is a direct transcriptional target of MYCN.

Materials and Methods

Immunohistochemistry of neuroblastoma tumors. Eighty-two formalin-fixed, paraffin-embedded diagnostic, untreated neuroblastoma tumors were examined for p53 and MYCN by immunohistochemistry using antibodies and methods previously reported (12). MYCN hybridoma supernatant MYCN (NCMIX102) was used at a 1:4 dilution. Positive tissue controls included colonic adenocarcinoma for p53 and *MYCN*-amplified NGP neuroblastoma cell cytoblocks for MYCN. Negative controls included incubations without primary antibodies and surrounding nontumor tissue. The p53 and MYCN labeling indices were performed as previously described (12). *MYCN* amplification was performed routinely on 40 frozen tumors, which were diagnosed after 1990, using Southern blot hybridization and fluorescent *in situ* hybridization.

Cell lines. p53 wild-type neuroblastoma cell lines (18, 19) used were *MYCN*-amplified (IMR32, NBLW, CHLA136, LAN5, SMSKCNR, and NGP), non–*MYCN*-amplified (SHSY5Y, NB69, SKNRA, and SHEP), non–*MYCN*-amplified high MYCN expressing (SJNB1 and NBLS), and the conditional MYCN-expressing SHEP Tet21N system together with p53-null osteosarcoma SAOS2 and p53 mutant neuroblastoma SKNBE2C cells (20). Cells were cultured as previously described (21). To switch off MYCN expression, Tet21N cells were cultured in the presence of 1 μg/mL of tetracycline (Sigma) for 48 h. Cell lines were obtained from the Children's Oncology Group Cell Culture and Xenograft Repository (LAN5), Sue Cohn (NBLW and NBLS), Linda Harris (SJNB1), Penny Lovat (SHSY5Y, SHEP, and IMR32), John Maris (NB69), Patrick Reynolds (SKNRA, SMSKCNR, and CHLA136), Barbara Spengler (SKNBE2C), Manfred Schwab (SHEPTet21N), Rogier Versteeg (NGP), and Ximena Montano (SAOS2) between 1996 and 2007, and were validated upon receipt using cytogenetic analysis courtesy of Nick Bown, Institute of Human Genetics, Newcastle University, Framlington Place, Newcastle upon Tyne, United Kingdom.

Quantitative reverse transcription PCR. Quantitative reverse transcription PCR (qRT-PCR) was performed as previously described (21). All primers and probes were inventoried TaqMan Gene Expression Assays (Applied Biosystems). RNA expression values were normalized to actin. All experiments were performed in triplicate.

Western analysis. Western blotting was performed using previously described methods (20). Primary antibodies used were p53 DO-7 (Novocastra Laboratories, Ltd.) at 1:1,000, MYCN (NCMII100) at 1:100, actin (Sigma) at 1:500, MDM2 (Calbiochem) at 1:100, $p21^{WAF1}$ (Calbiochem) at 1:100, phosphorylated p53 (Ser^{15}) at 1:1,000, cleaved caspase-3 (Cell Signaling Technology, Inc.) at 1:1,000, and PUMA (Calbiochem) at 1:300.

Secondary goat anti-mouse/rabbit horseradish peroxidase–conjugated antibody (Dako) was used at 1:500. Densitometry was performed as previously described (21) and expression normalized to actin.

Plasmids and luciferase assays. Plasmids used were the p53-dependent pGL3-P2 reporter construct (22),

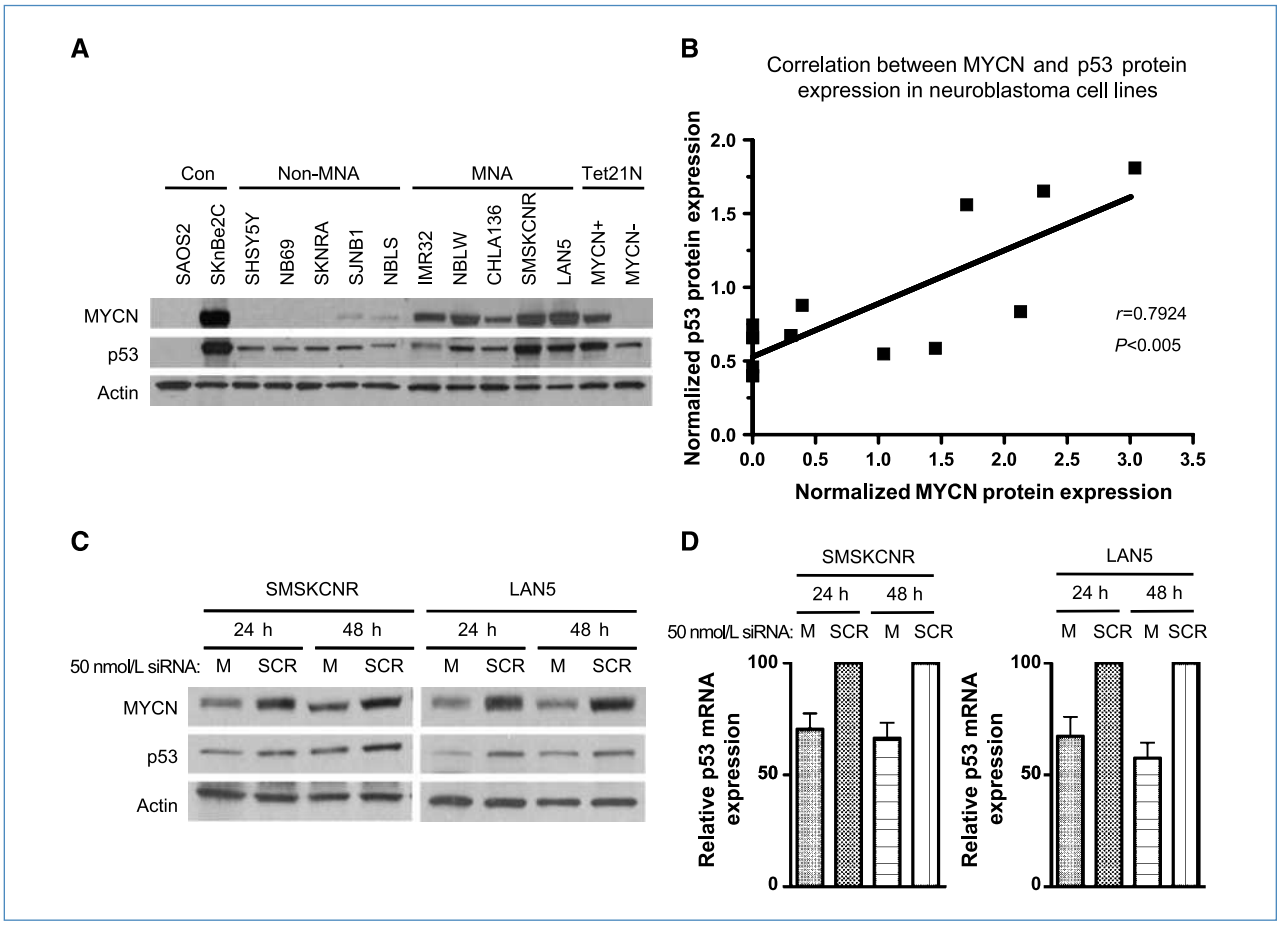

Figure 2. p53 expression correlates with *MYCN* status and expression in neuroblastoma cell lines. A, Western blot showing p53 and MYCN protein expression in neuroblastoma cell lines (Con, control). B, correlation between p53 protein and MYCN protein expression in neuroblastoma cell lines (Spearman correlation, $r = 0.7924$, $P < 0.005$). p53 and MYCN expression was determined using densitometry, and normalized to actin. Knockdown of MYCN expression using siRNA (50 nmol/L; M) in two *MYCN*-amplified neuroblastoma cell lines, SMSKCNR and LAN5, compared with scrambled siRNA (SCR) led to decreased p53 protein expression (C) and mRNA expression (D) in both cell lines.

pCMV-β-galactosidase (Stratagene), pRenilla-TK vector (Promega), and p53 promoter reporter constructs pGL2-200 bp and pGL2-356 bp originally described by Wang and El-Deiry (23) and purchased from Addgene (Addgene). pGL2-Δ200 bp and pGL2-Δ356 bp were generated by replacing the E-Box CATGTG with CTGCAG, and confirmed by sequencing. The pCMV14-MYCN expression plasmid was generated by cloning the CDS of MYCN into the p3XFLAG-CMV-14 vector (Sigma). Cells were transfected using FuGENE 6 (Roche) or polyethyleneimine (Sigma). Luciferase activity was measured as previously described (24) or by using the Dual-Luciferase Reporter Assay (Promega). To control for transfection efficiency, luciferase activity was normalized to β-galactosidase activity or Renilla luciferase activity. All experiments were performed in triplicate.

p53 DNA binding assay. The TransAM ELISA-based p53 transcription factor assay (Active Motif) was used according to the protocols of the manufacturer. Nuclear extracts were prepared using previously described methods (12), and 5 μg of protein used per well. Samples were prepared in triplicate and assayed in duplicate. Absorption was read at 450 nm with a reference wavelength of 655 nm.

Gene expression microarray. Cells were harvested from Tet21N MYCN– and Tet21N MYCN+ cells in triplicate and analyzed using Affymetrix U133 plus 2.0 oligonucleotide arrays. Arrays were performed at the CRUK Facility (Paterson Institute, Manchester, United Kingdom). Microarray data was analyzed using GeneSpring GX (Agilent Technologies Inc., Santa Clara, CA). Selected genes were validated using qRT-PCR. Array data is deposited in ArrayExpress, accession number E-MEXP-2340.

RNA interference. Short interfering RNAs (siRNA) were transfected into cells using LipofectAMINE (Invitrogen) to concentrations as indicated. siRNAs were purchased from Eurogentec (Eurogentec, Ltd.), using previously described sequences for p53 (25) and MYCN (21). All experiments were performed in triplicate.

Irradiation-induced DNA damage and caspase assays. Cells were treated with 4 Gy of X-irradiation from a RS320 irradiation system (Gulmay Medical). Cells were harvested

at the indicated times post-irradiation for protein analysis or caspase analysis. Experiments were performed in triplicate. Caspase-3/7 activity was measured using the Caspase-Glo 3/7 assay (Promega) according to the instructions of the manufacturer. Experiments were performed in triplicate.

Chromatin immunoprecipitation. Chromatin immunoprecipitation (ChIP) was performed as previously described (26), using 5 μg of anti-MYCN B8.4B, anti-Max C-17, or IgG (all from Santa Cruz Biotechnology, Inc.) as a negative control. Samples were analyzed using SYBR Green quantitative PCR with specific primers. Nucleolin was used as a positive control. Experiments were performed in triplicate. All primer sequences are listed in Supplementary Information Table S1.

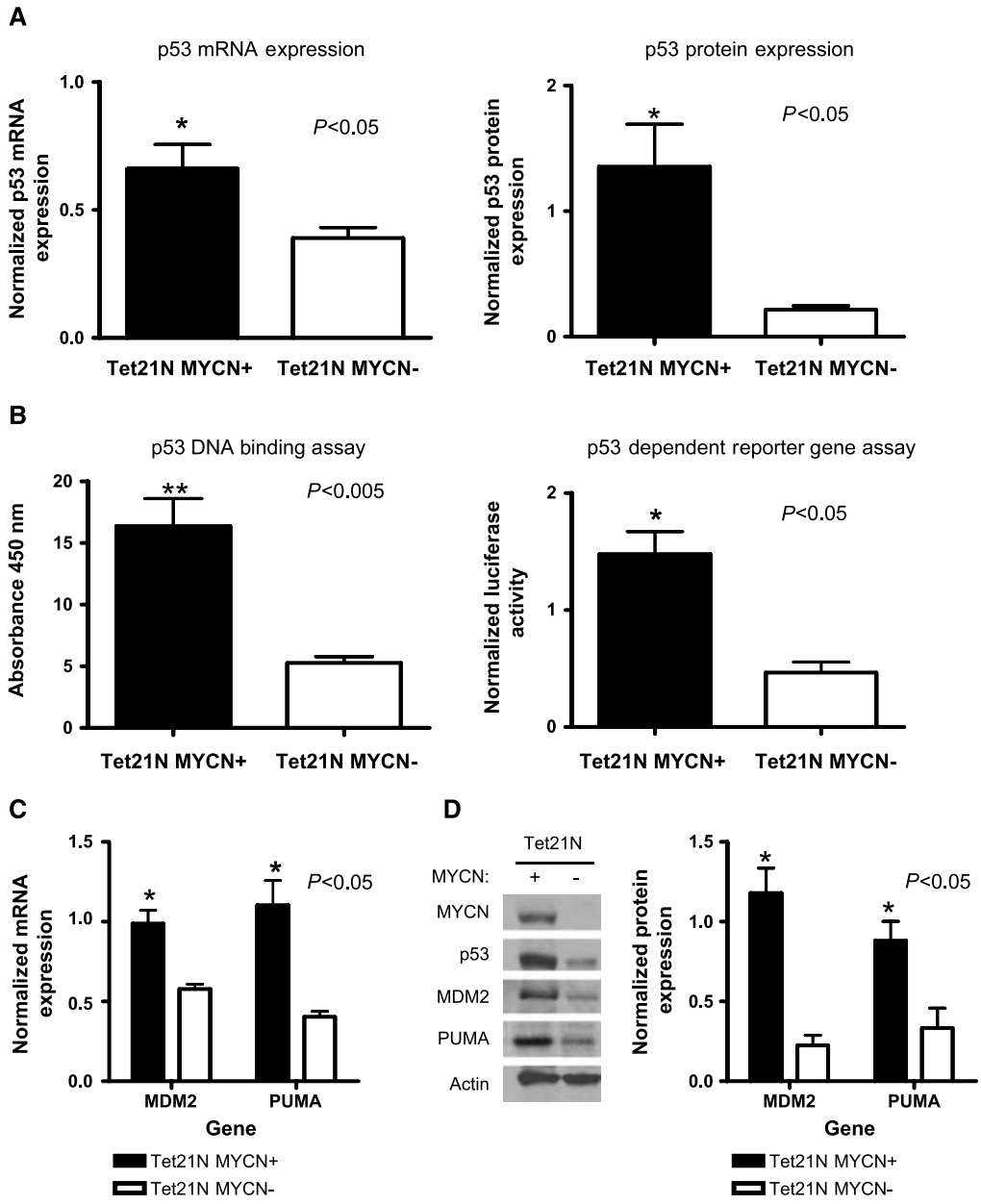

Figure 3. p53 mRNA and protein expression, and DNA binding and transcriptional activity in Tet21N cells. A, p53 mRNA (left) and protein expression (right) in the presence of MYCN (paired *t* test, $P < 0.05$). B, p53 DNA-binding capacity (left; paired *t* test, $P < 0.005$) and p53-dependent reporter gene activity (right; paired *t* test, $P < 0.05$) in the presence of MYCN. The luciferase activity of the p53-dependent pGL3-P2 reporter construct was normalized to β-galactosidase activity of pCMV-β-galactosidase plasmid construct. C, bar chart showing higher mRNA expression of p53 target genes MDM2 and PUMA in the presence of MYCN (paired *t* test, $P < 0.05$). D, Western blot (left) and densitometry analysis (right) normalized to actin showing higher protein expression of p53 target genes MDM2 and PUMA in the presence of MYCN (paired *t* test, $P < 0.05$).

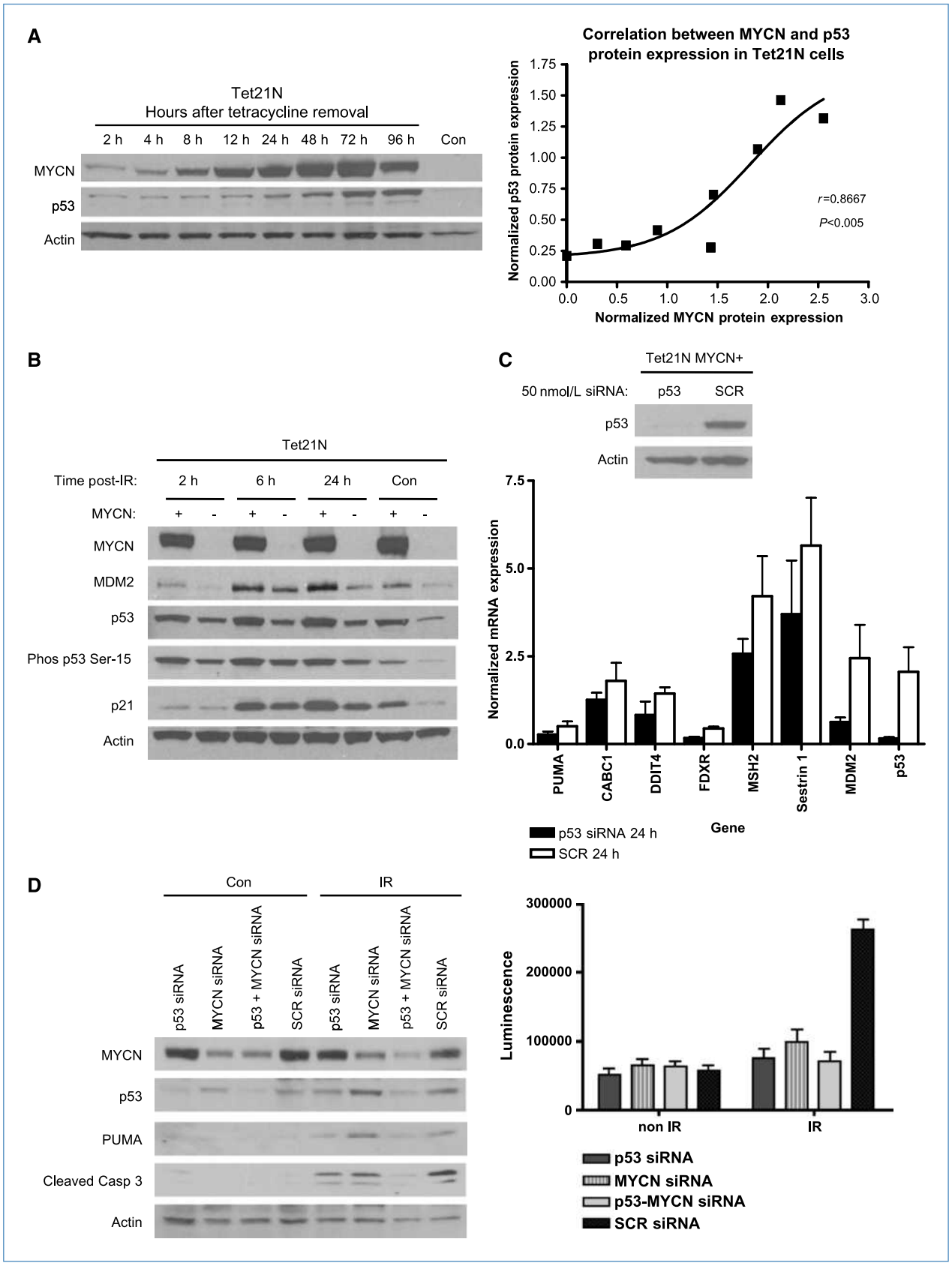
A
Tet21N
Hours after tetracycline removal
2 h 4 h 8 h 12 h 24 h 48 h 72 h 96 h Con
MYCN
p53
Actin
Correlation between MYCN and p53 protein expression in Tet21N cells
Normalized p53 protein expression
Normalized MYCN protein expression
r=0.8667
P<0.005
B
Tet21N
Time post-IR: 2 h 6 h 24 h Con
MYCN: + - + - + - + -
MYCN
MDM2
p53
Phos p53 Ser-15
p21
Actin
C
Tet21N MYCN+
50 nmol/L siRNA: p53 SCR
p53
Actin
Normalized mRNA expression
PUMA
CABC1
DDIT4
FDXR
MSH2
Sestrin 1
MDM2
p53
Gene
p53 siRNA 24 h
SCR 24 h
D
Con
IR
p53 siRNA
MYCN siRNA
p53 + MYCN siRNA
SCR siRNA
MYCN
p53
PUMA
Cleaved Casp 3
Actin
Luminescence
non IR
IR
p53 siRNA
MYCN siRNA
p53-MYCN siRNA
SCR siRNA

Actinomycin D and cycloheximide treatment. Tet21N MYCN+ and MYCN− cells were treated with either 1 μg/mL of actinomycin D (Sigma), or 25 μmol/L of cycloheximide (Calbiochem). Cells were harvested at the indicated times after actinomycin D treatment for qRT-PCR analysis of mRNA expression, and after cycloheximide treatment for protein analysis. Experiments were performed in triplicate.

Statistical analyses. Statistical tests were performed using Minitab (Minitab, Inc.) or GraphPad Prism (GraphPad Software, Inc.). All statistical tests were two-sided. If the expected frequency of a χ^2 test was <5, Fisher's exact test was performed using GraphPad Prism.

Results

p53 protein expression is associated with MYCN amplification and expression in neuroblastoma tumors. p53 expression, localization, and relationship with histology in this set of neuroblastoma tumors has been previously reported (12). p53 was found to be predominantly nuclear and expressed at high levels in undifferentiated and poorly differentiated neuroblastoma (Fig. 1A; ref. 12). MYCN expression was nuclear, heterogeneous, and expressed at higher levels in undifferentiated, poorly differentiated, and International Neuroblastoma Pathology Classification unfavorable histology tumors (Fig. 1A; data not shown). MYCN was not expressed in Schwannian stroma (Fig. 1A). MYCN expression was significantly higher in *MYCN*-amplified tumors as expected and only three non–*MYCN*-amplified tumors expressed MYCN detectable by immunohistochemistry (Fig. 1A and B; Table 1). Using the median labeling index for p53 and MYCN in all 82 tumors as a cutoff between positive and negative expression, increased p53 expression was significantly associated with *MYCN* amplification with two of the p53 antibodies used (Table 1; Fig. 1A and C), and with MYCN expression with all three p53 antibodies (Table 1; Fig. 1A and D). For p53DO-7, the median difference in labeling index between *MYCN*-amplified and nonamplified neuroblastoma was 8.6%, median p53DO-7 labeling indices were 6.7% for non–*MYCN*-amplified tumors and 13.5% for *MYCN*-amplified tumors (Fig. 1C).

p53 protein expression correlates with* MYCN *expression in neuroblastoma cell lines. p53 protein levels were analyzed in a panel of 10 p53 wild-type neuroblastoma cell lines, conditional MYCN expressing SHEP Tet21N cells, and two negative control cell lines, p53 mutant SKNBE2C and p53 null SAOS2 cells (Fig. 2A). Induced levels of MYCN in Tet21N MYCN+ cells were comparable with *MYCN*-amplified neuroblastoma cell lines (Fig. 2A). p53 expression was found to correlate with MYCN expression ($P < 0.005$, $r = 0.7924$, Spearman correlation; Fig. 2A and B), but not with *MYCN* amplification (data not shown).

To further investigate p53 expression in relation to MYCN expression, MYCN expression was inhibited using siRNA in p53 wild-type *MYCN*-amplified SMSKCNR and LAN5 cells. This led to decreased p53 protein (Fig. 2C) and mRNA expression (Fig. 2D) in both cell lines. At 24 hours after MYCN knockdown, LAN5 cells exhibited a ~40% reduction in p53 mRNA expression (Fig. 2D) and a ~50% reduction in p53 protein expression ($P < 0.05$, paired t test; Fig. 2C), whereas the SMSKCNR cell line exhibited a ~30% (Fig. 2D) and ~40% (Fig. 2C) reduction in p53 mRNA and protein expression, respectively.

p53 expression, transcriptional activity, and induction of p53-regulated genes in SHEP Tet21N cells. Tet21N MYCN+ cells were found to express significantly higher p53 mRNA ($P < 0.05$, paired t test; Fig. 3A) and protein ($P < 0.05$, paired t test; Figs. 2A and 3A) compared with Tet21N MYCN− cells. Consistent with higher p53 transcript and protein levels, Tet21N MYCN+ cells exhibited significantly greater p53 DNA-binding capacity ($P < 0.005$, paired t test) and transcriptional activity ($P < 0.05$, paired t test; Fig. 3B) in comparison with Tet21N MYCN− cells. Furthermore, higher mRNA ($P < 0.05$, paired t test; Fig. 3C) and protein ($P < 0.05$, paired t test; Fig. 3D) expression of two endogenous p53 target genes, *MDM2* and *PUMA*, were observed in Tet21N MYCN+ cells compared with Tet21N MYCN− cells, confirming the results of the reporter gene and DNA binding assays, indicating that the accumulated p53 in Tet21N MYCN+ cells is transcriptionally active.

Modulation of MYCN expression in Tet21N cells by continuous culture in the presence of tetracycline for 2 weeks, followed by the removal of tetracycline from the growth medium, resulted in the induction of MYCN expression and showed that p53 mRNA (data not shown) and protein expression positively correlated with MYCN protein expression ($P < 0.005$, $r = 0.8667$, Spearman correlation; Fig. 4A), lending further support for MYCN regulation of p53 in this system.

To determine whether p53 is functional after DNA damage in Tet21N MYCN+/− cells, cells were subjected to 4 Gy of X-irradiation and analyzed for the expression of $p21^{WAF1}$ and MDM2. Following DNA damage, there was an increase in Ser^{15} phosphorylated p53 as well as induction of p53,

Figure 4. p53 expression in the presence of MYCN is functional after DNA damage, and necessary for apoptosis. A, Western blot (left) and representative graph (right) of the positive correlation between MYCN protein and p53 protein expression in Tet21N cells harvested after tetracycline removal from growth medium (Spearman correlation, $r = 0.7924$, $P < 0.005$). Con, cells cultured continuously in the presence of tetracycline. B, Western analysis showing that p53 is functional in both Tet21N MYCN+ and MYCN− cells after DNA damage, leading to induction of target genes $p21^{WAF1}$ and MDM2. Con, nonirradiated samples. C, qRT-PCR analysis of seven p53-regulated genes identified using microarray analysis, upregulated in the presence of MYCN and showed a decrease in expression after p53 siRNA treatment (50 nmol/L) for 24 h. D, *MYCN*-amplified NGP cells treated with MYCN siRNA (40 nmol/L), p53 siRNA (50 nmol/L), p53 and MYCN siRNA (35 nmol/L of each siRNA), or SCR siRNA (70 nmol/L) for 48 h prior to irradiation-induced DNA damage. Twenty-four hours post-irradiation, cells were harvested and analyzed for the expression of apoptosis mediators cleaved caspase-3 and PUMA (left) and caspase-3/7 activity (right).

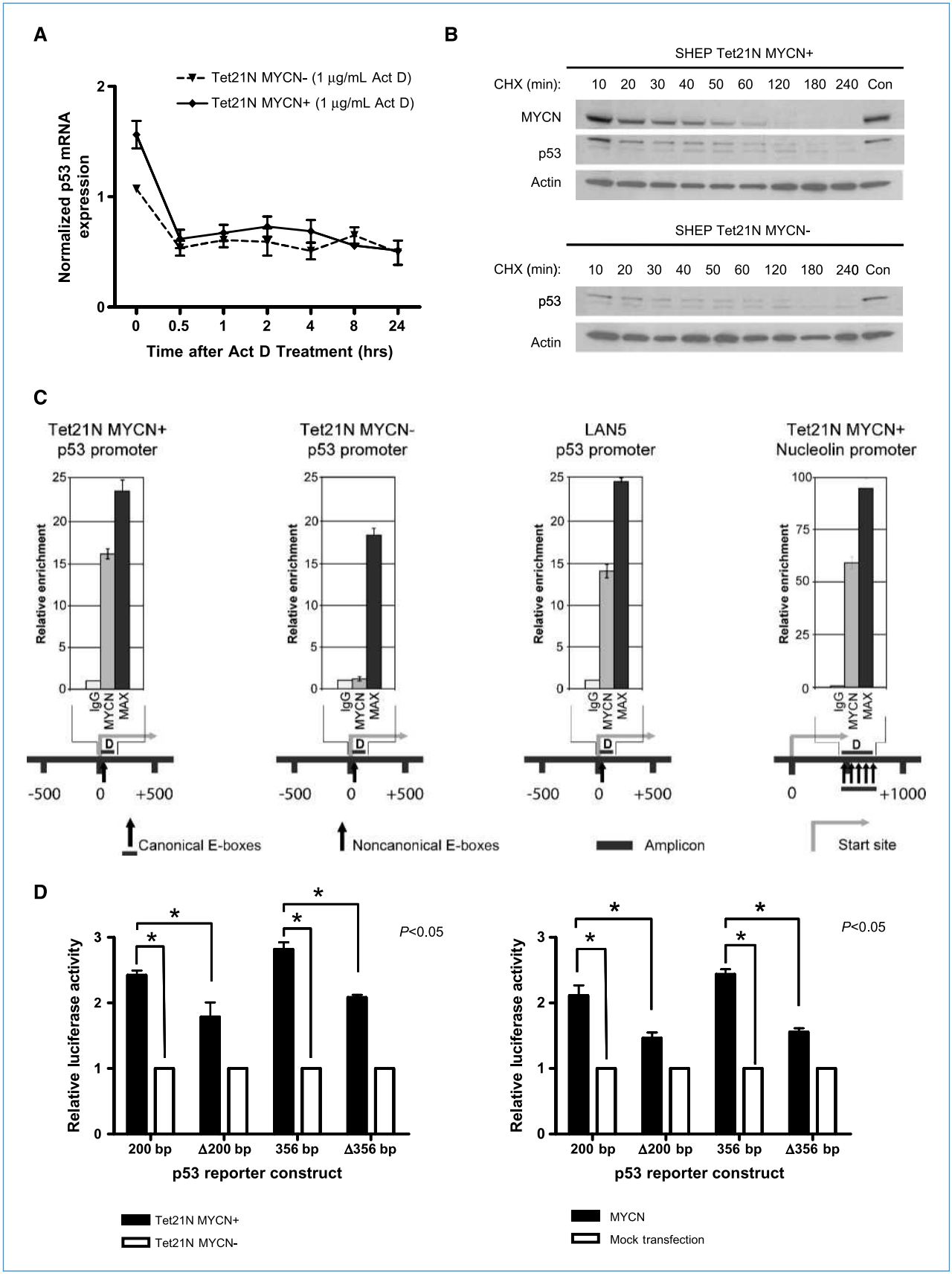
A
Tet21N MYCN- (1 μg/mL Act D)
Tet21N MYCN+ (1 μg/mL Act D)
Normalized p53 mRNA expression
Time after Act D Treatment (hrs)
B
SHEP Tet21N MYCN+
CHX (min): 10 20 30 40 50 60 120 180 240 Con
MYCN
p53
Actin
SHEP Tet21N MYCN-
CHX (min): 10 20 30 40 50 60 120 180 240 Con
p53
Actin
C
Tet21N MYCN+ p53 promoter
Tet21N MYCN- p53 promoter
LAN5 p53 promoter
Tet21N MYCN+ Nucleolin promoter
Relative enrichment
IgG
MYCN
MAX
Canonical E-boxes
Noncanonical E-boxes
Amplicon
Start site
D
Relative luciferase activity
P<0.05
200 bp
Δ200 bp
356 bp
Δ356 bp
p53 reporter construct
Tet21N MYCN+
Tet21N MYCN-
MYCN
Mock transfection

$p21^{WAF1}$, and MDM2 in Tet21N MYCN+ and MYCN− cells (Fig. 4B). The basal and induced levels of p53, phosphorylated p53 at Ser^{15}, MDM2, and $p21^{WAF1}$ were all higher in Tet21N MYCN+ cells compared with Tet21N MYCN− cells (Fig. 4B), consistent with higher levels of p53 activity in the presence of MYCN. The above data confirms that p53 is functional both in the presence and absence of MYCN in this system.

To determine whether the greater induction of $p21^{WAF1}$ and MDM2 in Tet21N MYCN+ cells is dependent on functional p53, p53 was knocked down using siRNA and the cells treated with 4 Gy of X-irradiation prior to analysis of $p21^{WAF1}$ and MDM2 expression. Inhibition of p53 using siRNA led to complete abrogation of $p21^{WAF1}$ and MDM2 induction following DNA damage, further confirming that p53 is functional and that induction of $p21^{WAF1}$ and MDM2 is dependent on functional p53 (data not shown). In addition, following knockdown of p53, basal levels of MDM2 and $p21^{WAF1}$ were much lower than in the cells treated with scrambled (SCR) control siRNA (data not shown).

***Gene expression microarray analysis of p53 and p53-regulated gene expression in the presence of ectopic* MYCN.** Affymetrix gene expression microarray analysis of SHEP Tet21N MYCN+ and MYCN− cells was performed to determine whether there was upregulation of p53 and/or p53-regulated genes in the presence of MYCN. qRT-PCR was performed on selected genes to validate microarray results (data not shown), and the results were consistent. Several previously reported putative MYCN target genes were found to be differentially expressed in the presence of MYCN (Supplementary Table S2). In agreement with qRT-PCR analysis, p53 transcript expression detected by microarray analysis was upregulated 1.9-fold in the presence of MYCN (Supplementary Table S3). In addition, many p53-regulated genes were also found to be differentially upregulated in the presence of MYCN (Supplementary Table S3 and Supplementary Fig. S1). To confirm that the increased expression of p53-regulatable genes in the presence of MYCN was p53-dependent, p53 expression in the Tet21N MYCN+ cells was inhibited using siRNA, and selected p53-regulated genes analyzed by qRT-PCR (Fig. 4C). All genes tested showed a decrease in transcript expression in the presence of p53 siRNA compared with SCR control, confirming that the observed increase in expression of p53-regulatable genes is at least in part dependent on higher levels of p53 present in Tet21N MYCN+ cells (Fig. 4C).

Irradiation-induced apoptosis in MYCN-amplified cells is dependent on p53. To determine whether higher levels of apoptosis in *MYCN*-amplified neuroblastoma cells is dependent on higher levels of p53 in the presence of MYCN, *MYCN*-amplified NGP cells were treated with MYCN and/or p53 siRNA or SCR siRNA prior to irradiation-induced DNA damage (Fig. 4D). NGP cells were chosen because we have previously reported high levels of apoptosis following irradiation in this cell line (20). Apoptosis was determined by analysis of expression of apoptosis mediator PUMA and cleavage of caspase-3 together with quantification of caspase-3/7 activity. Twenty-four hours after irradiation, inhibition of MYCN or p53 led to decreased caspase-3/7 activity, compared with cells treated with SCR siRNA (Fig. 4D). Furthermore, inhibition of MYCN and p53 led to a slightly greater reduction in caspase-3/7 activity than inhibition of MYCN or p53 alone (Fig. 4D). Similarly, inhibition of MYCN and p53 led to a greater reduction in cleavage of caspase-3 and less induced PUMA than inhibition of MYCN or p53 alone (Fig. 4D).

p53 regulation is predominantly at the level of transcription. To determine whether the increased p53 expression in the presence of MYCN is due to transcriptional regulation or protein stabilization through posttranslational modifications, Tet21N cells were treated with either 1 μg/mL of actinomycin D or 25 μmol/L of cycloheximide. Actinomycin D (Fig. 5A) and cycloheximide (Fig. 5B) treatment led to decreases in p53 mRNA and protein levels, respectively, in both Tet21N MYCN+ and MYCN− cells. p53 was found to have a half-life of 30 to 40 minutes in this system. MYCN levels also decreased following cycloheximide treatment (Fig. 5B). The above data suggests that the increased expression of p53 in the presence of MYCN is predominantly via transcriptional regulation rather than p53 stabilization by posttranslational modifications.

***p53 is a direct transcriptional target of* MYCN.** MYCN ChIP was performed in two *MYCN*-amplified neuroblastoma cell lines and the Tet21N system to determine whether MYCN can directly bind to an E-Box motif within the p53 promoter *in vivo*. It was found that MYCN binds directly to the noncanonical E-Box motif located close to the transcriptional start site of p53 in Tet21N MYCN+ cells (Fig. 5C) and *MYCN*-amplified neuroblastoma cell lines LAN5 (Fig. 5C) and SKNBE2C (Supplementary Fig. S2). As expected, no MYCN binding was observed in Tet21N MYCN− cells (Fig. 5C). MYCN binding to the E-Box within the nucleolin promoter in Tet21N MYCN+ cells was used as a positive control (Fig. 5C).

To confirm the functional regulation of p53 by MYCN, p53 reporter constructs incorporating the wild-type E-Box motif, CATGTG (pGL2-200 bp and pGL2-356 bp), or the mutated E-Box motif, CTGCAG (pGL2-Δ200 bp and pGL2-Δ356 bp)

Figure 5. MYCN predominantly regulates p53 at the transcriptional level via direct binding to the E-Box motif within the p53 promoter. A, qRT-PCR analysis of p53 mRNA expression in Tet21N MYCN+ and MYCN− cells after treatment with 1 μg/mL of actinomycin D shows a decrease in p53 mRNA expression, suggesting that MYCN regulates p53 transcription. B, Western blot showing p53 and MYCN protein expression in Tet21N MYCN+ (top) and MYCN− cells (bottom) harvested after treatment with 25 μmol/L of cycloheximide (CHX) shows a decrease in p53 expression suggesting that p53 is not predominantly posttranslationally stabilized. C, MYCN ChIP analysis of the p53 promoter in Tet21N MYCN+ cells (left), Tet21N MYCN− cells (second from left), and *MYCN*-amplified LAN5 cells (second from right). As a positive control, direct binding of MYCN to the nucleolin promoter in Tet21N MYCN+ cells (right). D, relative luciferase activity of p53 promoter constructs (pGL2-200 bp, pGL2-Δ200 bp, pGL2-356 bp, pGL2-Δ356 bp) transfected into Tet21N MYCN+ and MYCN− cells (left), and cotransfected with pCMV14-MYCN expression plasmid into SHEP cells (right).

were transfected into Tet21N MYCN+ and Tet21N MYCN− cells, and also cotransfected with the pCMV14-MYCN expression plasmid into parental SHEP cells. In line with the above ChIP data, p53 promoter constructs incorporating the wild-type E-Box motif exhibited significantly greater luciferase activity in the presence of MYCN ($P < 0.05$, paired t test; Fig. 5D) in Tet21N cells as well as in SHEP cells cotransfected with pCMV14-MYCN ($P < 0.05$, paired t test; Fig. 5D). Mutation of the E-Box motif led to significantly reduced luciferase activity ($P < 0.05$, paired t test) in Tet21N MYCN+ cells (Fig. 5D) as well as in SHEP cells cotransfected with pCMV14-MYCN ($P < 0.05$, paired t test; Fig. 5D).

Discussion

Like c-MYC, MYCN plays a paradoxical role in driving both cellular proliferation (27) and inducing apoptosis (28–30). This is observed histologically by a high mitosis-karyorrhexis index in both human *MYCN*-amplified neuroblastoma tumors (31–34) and *MYCN* transgenic mouse neuroblastoma tumors (35). In addition, in transgenic mouse tumors, we reported tingible body macrophages reflecting high levels of apoptosis within these tumors (35). Studies using *MYCN*-amplified cell lines, *MYCN* transgenic mouse tumors and ectopic MYCN expressing Tet21N cells have shown higher p53 levels in the presence of MYCN (21, 36, 37) and increased levels of apoptosis in response to chemotherapeutic agents (28, 38–40), and irradiation (21).

We and others have previously observed wild-type nuclear functional p53 accumulation in neuroblastoma cell lines (reviewed in ref. 10) and tumors (12). p53 has been shown to be a direct target gene of c-MYC, in which the p53 promoter has been reported to contain an E-Box–related sequence (CATGTG) through which the *Myc* gene family exert transcriptional activity (13, 14). We hypothesized that p53 accumulation in neuroblastoma is related to *MYCN* amplification and expression and that p53 is a direct transcriptional target of MYCN in neuroblastoma.

Here, we show that p53 protein expression correlates with MYCN protein expression in both primary neuroblastoma tumors and neuroblastoma cell lines. Using a regulatable MYCN expression system, p53 was found to be functional and exhibited greater transcriptional activity in the presence of MYCN leading to increased expression of several p53 target genes. Using quantitative MYCN ChIP, MYCN was found to bind directly to the noncanonical E-Box motif (CATGTG) within the p53 promoter *in vivo*, and using reporter gene assays, direct functional upregulation of transcription from the p53 promoter by MYCN was shown. Furthermore, deletion of this E-Box led to reduced transcriptional activity from the p53 promoter by MYCN. This data provides strong support to the model that this specific E-Box is responsible for MYCN-mediated regulation of p53. The binding of MYCN to an E-Box within the p53 promoter has very recently been reported using ChIP-chip arrays (7), however, this study did not include the functional upregulation of p53. Taken together, these findings provide an important and direct mechanism by which MYCN is able to sensitize cells for p53-mediated apoptosis.

Our data is both consistent with and provides a direct mechanism to account for previous studies which have shown that *MYCN*-amplified neuroblastoma tumors expressed significantly higher levels of p53 RNA in comparison with nonamplified tumors (7, 41, 42). It is also possible that the association of p53 with undifferentiated, highly proliferative neuroblastoma we previously reported is mediated through MYCN (12), and that MYCN may be involved in other studies linking p53 RNA expression with unfavorable neuroblastoma (43).

Our data is also in line with work in the TH-*MYCN* transgenic mouse model which showed that MYCN-driven tumor formation had higher penetrance and reduced latency in p53 haploinsufficient mice, and that chemotherapy-induced apoptosis was shown to be p53-dependent, in which apoptosis was significantly reduced in TH-*MYCN* p53+/− tumors compared with p53+/+ tumors (40).

Mechanisms by which members of the *Myc* family induce apoptosis are not fully understood (reviewed in ref. 44). One mechanism is via $p14^{ARF}$-mediated increased p53 expression, stability, and activity (45), although we have previously reported that SHEP cells are homozygously deleted for $p14^{ARF}$ (18), and this was further confirmed in the present study (data not shown). However, $p14^{ARF}$ might be involved in other neuroblastoma cell lines in addition, or instead of, direct regulation of the p53 gene shown in the present study.

MYCN and p53 are both expressed in the normal embryonic developing nervous system, during the phase of precursor cell expansion prior to the onset of differentiation. In the context of normal embryonic development, the present findings therefore provide a mechanism for MYCN-driven p53-dependent apoptosis, which may be important in eliminating any rapidly proliferating neuroblasts exposed to potential teratogens to prevent deregulated proliferation and aberrations during development.

Our findings might help to explain why neuroblastomas are initially chemosensitive; however, despite an initial response, more than half of all cases relapse with chemoresistant disease, suggesting that *MYCN*-amplified tumors eventually develop mechanisms to evade MYCN-driven apoptosis (reviewed in ref. 9). There is evidence from cell line studies that *MYCN*-amplified cell lines may circumvent MYCN-driven p53-dependent apoptosis by selecting for cells with aberrations in the p53/MDM2/$p14^{ARF}$ pathway. Analysis of neuroblastoma cell lines reported to date with aberrations in the p53/MDM2/$p14^{ARF}$ pathway show that 25 of 34 (74%) cell lines are *MYCN*-amplified (Supplementary Information, Table S4) and predominantly established following previous therapy at relapse (18), when abnormalities of the p53 pathway in neuroblastoma tumors have been previously reported (reviewed in ref. 10). A study examining the p53 pathway in relapsed *MYCN*-amplified neuroblastomas is warranted.

Further illustrating the complexity of the paradoxical role of MYCN in proliferation and apoptosis, MDM2, the critical negative regulator of p53, has previously been reported to be

a direct target of MYCN (46). In the present study, siRNA-mediated inhibition of p53 led to a decrease in MDM2 expression (data not shown), suggesting that increased expression of MDM2 in the presence of MYCN may also be dependent on the higher expression of p53 and not solely due to direct upregulation by MYCN.

In conclusion, this study provides several lines of evidence that p53 is a direct transcriptional target of MYCN in neuroblastoma and is likely to be a mechanism for MYCN-induced p53-dependent apoptosis. However, the various selection pressures on *MYCN*-amplified tumors either spontaneously or via chemotherapy may lead to selection for those cells that can evade apoptosis by various mechanisms which result in *MYCN*-amplified neuroblastoma progressing to become such a severe phenotype.

Disclosure of Potential Conflicts of Interest

No potential conflicts of interest were disclosed.

Acknowledgments

We thank the following for providing cell lines: Sue Cohn, Linda Harris, Penny Lovat, John Maris, Patrick Reynolds, Barbara Spengler, Manfred Schwab, and Ximena Montano. We also thank Naohiko Ikegaki for the MYCN antibodies, Ximena Montano for the p53 DO-1 antibody, and Novocastra, Newcastle upon Tyne, for the p53DO-7 and Pab1801 antibodies used for immunohistochemistry. We are also grateful to Nick Bown, Angela Baker, and Julian Board for MYCN analyses; Allison Carpenter, Christine Estlin, Janet Thompson, and Susan Wood for pathology technical support; Donatella Manzoni for assistance with cell culture; and Dan Swan for bioinformatics support.

Grant Support

Cancer Research UK, The North of England Children's Cancer Research Fund, the U.K. Department of Health, the Italian Association for Cancer Research, and the Italian Ministry of Research and Education.

The costs of publication of this article were defrayed in part by the payment of page charges. This article must therefore be hereby marked *advertisement* in accordance with 18 U.S.C. Section 1734 solely to indicate this fact.

Received 7/15/09; revised 11/17/09; accepted 12/2/09; published OnlineFirst 2/9/10.

References

1. Matthay KK, Reynolds CP, Seeger RC, et al. Long-term results for children with high-risk neuroblastoma treated on a randomized trial of myeloablative therapy followed by 13-cis-retinoic acid: a Children's Oncology Group study. J Clin Oncol 2009;27:1007–13.
2. Pearson AD, Pinkerton CR, Lewis IJ, Imeson J, Ellershaw C, Machin D. High-dose rapid and standard induction chemotherapy for patients aged over 1 year with stage 4 neuroblastoma: a randomised trial. Lancet Oncol 2008;9:247–56.
3. Cohn SL, Tweddle DA. MYCN amplification remains prognostically strong 20 years after its "clinical debut". Eur J Cancer 2004;40:2639–42.
4. Grandori C, Eisenman RN. Myc target genes. Trends Biochem Sci 1997;22:177–81.
5. Zeller KI, Jegga AG, Aronow BJ, O'Donnell KA, Dang CV. An integrated database of genes responsive to the Myc oncogenic transcription factor: identification of direct genomic targets. Genome Biol 2003;4:R69.
6. Ben-Yosef T, Yanuka O, Halle D, Benvenisty N. Involvement of Myc targets in c-myc and N-myc induced human tumors. Oncogene 1998;17:165–71.
7. Westermann F, Muth D, Benner A, et al. Distinct transcriptional MYCN/c-MYC activities are associated with spontaneous regression or malignant progression in neuroblastomas. Genome Biol 2008;9:R150.
8. Laurenti E, Varnum-Finney B, Wilson A, et al. Hematopoietic stem cell function and survival depend on c-Myc and N-Myc activity. Cell Stem Cell 2008;3:611–24.
9. Hogarty MD. The requirement for evasion of programmed cell death in neuroblastomas with MYCN amplification. Cancer Lett 2003;197:173–9.
10. Tweddle DA, Pearson AD, Haber M, et al. The p53 pathway and its inactivation in neuroblastoma. Cancer Lett 2003;197:93–8.
11. Davidoff AM, Pence JC, Shorter NA, Iglehart JD, Marks JR. Expression of p53 in human neuroblastoma- and neuroepithelioma-derived cell lines. Oncogene 1992;7:127–33.
12. Chen L, Malcolm AJ, Wood KM, et al. p53 is nuclear and functional in both undifferentiated and differentiated neuroblastoma. Cell Cycle 2007;6:2685–96.
13. Reisman D, Elkind NB, Roy B, Beamon J, Rotter V. c-Myc trans-activates the p53 promoter through a required downstream CACGTG motif. Cell Growth Differ 1993;4:57–65.
14. Roy B, Beamon J, Balint E, Reisman D. Transactivation of the human p53 tumor suppressor gene by c-Myc/Max contributes to elevated mutant p53 expression in some tumors. Mol Cell Biol 1994;14:7805–15.
15. Hermeking H, Eick D. Mediation of c-Myc-induced apoptosis by p53. Science 1994;265:2091–3.
16. Blackwell TK, Huang J, Ma A, et al. Binding of myc proteins to canonical and noncanonical DNA sequences. Mol Cell Biol 1993;13:5216–24.
17. Reisman D, Loging WT. Transcriptional regulation of the p53 tumor suppressor gene. Semin Cancer Biol 1998;8:317–24.
18. Carr J, Bell E, Pearson AD, et al. Increased frequency of aberrations in the p53/MDM2/p14(ARF) pathway in neuroblastoma cell lines established at relapse. Cancer Res 2006;66:2138–45.
19. Tweddle DA, Malcolm AJ, Bown N, Pearson AD, Lunec J. Evidence for the development of p53 mutations after cytotoxic therapy in a neuroblastoma cell line. Cancer Res 2001;61:8–13.
20. Tweddle DA, Malcolm AJ, Cole M, Pearson AD, Lunec J. p53 cellular localization and function in neuroblastoma: evidence for defective G(1) arrest despite WAF1 induction in MYCN-amplified cells. Am J Pathol 2001;158:2067–77.
21. Bell E, Premkumar R, Carr J, et al. The role of MYCN in the failure of MYCN amplified neuroblastoma cell lines to G1 arrest after DNA damage. Cell Cycle 2006;5:2639–47.
22. Liang H, Lunec J. Characterisation of a novel p53 down-regulated promoter in intron 3 of the human MDM2 oncogene. Gene 2005;361:112–8.
23. Wang S, El-Deiry WS. p73 or p53 directly regulates human p53 transcription to maintain cell cycle checkpoints. Cancer Res 2006;66:6982–9.
24. Lu X, Vogt PK, Boger DL, Lunec J. Disruption of the MYC transcriptional function by a small-molecule antagonist of MYC/MAX dimerization. Oncol Rep 2008;19:825–30.
25. Armstrong JL, Veal GJ, Redfern CP, Lovat PE. Role of Noxa in p53-independent fenretinide-induced apoptosis of neuroectodermal tumours. Apoptosis 2007;12:613–22.
26. Weinmann AS, Farnham PJ. Identification of unknown target genes of human transcription factors using chromatin immunoprecipitation. Methods 2002;26:37–47.
27. Lutz W, Stohr M, Schurmann J, Wenzel A, Lohr A, Schwab M. Conditional expression of N-myc in human neuroblastoma cells increases expression of α-prothymosin and ornithine decarboxylase and accelerates progression into S-phase early after mitogenic stimulation of quiescent cells. Oncogene 1996;13:803–12.
28. Fulda S, Lutz W, Schwab M, Debatin KM. MycN sensitizes

neuroblastoma cells for drug-induced apoptosis. Oncogene 1999; 18:1479–86.
29. Aubry S, Charron J. N-Myc shares cellular functions with c-Myc. DNA Cell Biol 2000;19:353–64.
30. van Noesel MM, Pieters R, Voute PA, Versteeg R. The N-myc paradox: N-myc overexpression in neuroblastomas is associated with sensitivity as well as resistance to apoptosis. Cancer Lett 2003; 197:165–72.
31. Goto S, Umehara S, Gerbing RB, et al. Histopathology (International Neuroblastoma Pathology Classification) and MYCN status in patients with peripheral neuroblastic tumors: a report from the Children's Cancer Group. Cancer 2001;92:2699–708.
32. Shimada H, Stram DO, Chatten J, et al. Identification of subsets of neuroblastomas by combined histopathologic and N-myc analysis. J Natl Cancer Inst 1995;87:1470–6.
33. Shimada H, Ambros IM, Dehner LP, Hata J, Joshi VV, Roald B. Terminology and morphologic criteria of neuroblastic tumors: recommendations by the International Neuroblastoma Pathology Committee. Cancer 1999;86:349–63.
34. Altungoz O, Aygun N, Tumer S, Ozer E, Olgun N, Sakizli M. Correlation of modified Shimada classification with MYCN and 1p36 status detected by fluorescence *in situ* hybridization in neuroblastoma. Cancer Genet Cytogenet 2007;172:113–9.
35. Moore HC, Wood KM, Jackson MS, et al. Histological profile of tumours from MYCN transgenic mice. J Clin Pathol 2008;61:1098–103.
36. Sugihara E, Kanai M, Saito S, et al. Suppression of centrosome amplification after DNA damage depends on p27 accumulation. Cancer Res 2006;66:4020–9.
37. Cui H, Li T, Ding HF. Linking of N-Myc to death receptor machinery in neuroblastoma cells. J Biol Chem 2005;280:9474–81.
38. Fulda S, Lutz W, Schwab M, Debatin KM. MycN sensitizes neuroblastoma cells for drug-triggered apoptosis. Med Pediatr Oncol 2000;35:582–4.
39. Paffhausen T, Schwab M, Westermann F. Targeted MYCN expression affects cytotoxic potential of chemotherapeutic drugs in neuroblastoma cells. Cancer Lett 2007;250:17–24.
40. Chesler L, Goldenberg DD, Collins R, et al. Chemotherapy-induced apoptosis in a transgenic model of neuroblastoma proceeds through p53 induction. Neoplasia 2008;10:1268–74.
41. Berwanger B, Hartmann O, Bergmann E, et al. Loss of a FYN-regulated differentiation and growth arrest pathway in advanced stage neuroblastoma. Cancer Cell 2002;2:377–86.
42. Raschella G, Negroni A, Giubilei C, et al. Transcription of N-myc and proliferation-related genes is linked in human neuroblastoma. Cancer Lett 1991;56:45–51.
43. Ohira M, Oba S, Nakamura Y, et al. Expression profiling using a tumor-specific cDNA microarray predicts the prognosis of intermediate risk neuroblastomas. Cancer Cell 2005;7:337–50.
44. Adhikary S, Eilers M. Transcriptional regulation and transformation by Myc proteins. Nat Rev Mol Cell Biol 2005;6:635–45.
45. Zindy F, Eischen CM, Randle DH, et al. Myc signaling via the ARF tumor suppressor regulates p53-dependent apoptosis and immortalization. Genes Dev 1998;12:2424–33.
46. Slack A, Chen Z, Tonelli R, et al. The p53 regulatory gene MDM2 is a direct transcriptional target of MYCN in neuroblastoma. Proc Natl Acad Sci U S A 2005;102:731–6.